View metadata, citation and similar papers at core.ac.uk
brought to you by CORE
provided by Queensland University of Technology ePrints Archive

Published on 28 July 2011. Downloaded by Queensland University of Technology on 20/11/2013 23:06:48.

The active site behaviour of electrochemically synthesised gold nanomaterials†

Blake J. Plowman, Anthony P. O'Mullane* and Suresh K. Bhargava*

Received 11th February 2011, Accepted 3rd March 2011
DOI: 10.1039/c1fd00017a

Even though gold is the noblest of metals, a weak chemisorber and is regarded as being quite inert, it demonstrates significant electrocatalytic activity in its nanostructured form. It is demonstrated here that nanostructured and even evaporated thin films of gold are covered with active sites which are responsible for such activity. The identification of these sites is demonstrated with conventional electrochemical techniques such as cyclic voltammetry as well as a large amplitude Fourier transformed alternating current (FT-ac) method under acidic and alkaline conditions. The latter technique is beneficial in determining if an electrode process is either Faradaic or capacitive in nature. The observed behaviour is analogous to that observed for activated gold electrodes whose surfaces have been severely disrupted by cathodic polarisation in the hydrogen evolution region. It is shown that significant electrochemical oxidation responses occur at discrete potential values well below that for the formation of the compact monolayer oxide of bulk gold and are attributed to the facile oxidation of surface active sites. Several electrocatalytic reactions are explored in which the onset potential is determined by the presence of such sites on the surface. Significantly, the facile oxidation of active sites is used to drive the electroless deposition of metals such as platinum, palladium and silver from their aqueous salts on the surface of gold nanostructures. The resultant surface decoration of gold with secondary metal nanoparticles not only indicates regions on the surface which are rich in active sites but also provides a method to form interesting bimetallic surfaces.

Introduction

The gas and liquid phase heterogeneous catalytic behaviour of unsupported and supported gold has received significant attention since the discovery that gold when transformed from an often regarded inert bulk material to the nanostructured form demonstrates significant activity.[1–6] This is attributed to a variety of factors including size, shape, crystallographic orientation and interactions with an underlying support. Recently, nanosized gold has also attracted widespread attention in the field of electrochemistry with widespread applications as electrochemical sensors[7,8] and also as an effective electrocatalyst for fuel cell relevant reactions such as oxygen reduction and small organic molecule oxidation.[9–20]

However, it is interesting to note that gold is often regarded as a model electrode material for electrochemical studies. This is due to the well characterised behaviour of this metal in the bulk form in aqueous solution which exhibits a well defined double layer region that is considered to exhibit purely capacitive behaviour and

School of Applied Sciences, RMIT University, GPO Box 2476V, VIC, 3001, Australia. E-mail: anthony.omullane@rmit.edu.au; suresh.bhargava@rmit.edu.au

† Electronic supplementary information (ESI) available: See DOI: 10.1039/c1fd00017a

View Article Online

Published on 28 July 2011. Downloaded by Queensland University of Technology on 20/11/2013 23:06:48.

a monolayer oxide formation/removal process. Significantly however, the majority of electrocatalytic reactions that occur at a gold surface in aqueous solution are well within the double layer region with few reactions catalysed by the main oxide formation process.[14,21] Recently, it has been shown for gold and other metals including platinum, palladium, silver and copper that significant oxidation processes can occur within the double layer region of these metals which can be detected by the cyclic voltammetry technique once the electrode material has been sufficiently activated. This type of surface activation includes polarisation in the hydrogen evolution region,[22,23] multilayered oxide growth followed by removal,[24] repetitive potential cycling,[9] thermal treatments followed by rapid quenching[25] and sonochemical[26] methods. In all cases energy is inserted into the metal lattice which often results in the disruption of the outer layers of the metal to create an active surface. The creation of active sites, which are believed to consist of low lattice stabilised gold atoms, or clusters of atoms, are more readily oxidised compared to the bulk material where the atoms are fully lattice stabilised. This more facile oxidation of active gold results in significant electrochemical responses recorded in the double layer region. It is the creation of these low coordinated active sites which has been postulated to mediate electrocatalytic reactions of gold in aqueous solution.[21,27]

A further significant area of research has been the electrochemical synthesis of gold in the nanostructured form. This approach is advantageous in that it eliminates the need for organic species which are used as capping agents in chemical synthesis, and allows the bare metal to be investigated. This alleviates any problems associated with the influence that the capping species may have on the electrocatalytic reaction of interest or treatments that would be required for its removal which may also affect the surface chemistry of the metal. Using appropriate electrochemical protocols a wide variety of structures including flowers,[28] spikes,[29] rods,[30] pyramids,[31] spheres[32] and dendrites[33] can be produced which have been shown to possess good electrocatalytic and surface enhanced Raman scattering properties often attributed to the creation of active sites or hot spots. Even though the solution based electrochemical behaviour of nanoparticles has been well documented in terms of the observation of discrete single electron transfer processes[34–36] the standard electrochemical behaviour of immobilised nanostructures of gold on substrates in aqueous solution is often overlooked. This can offer a wealth of information regarding the effectiveness of such materials as an electrocatalyst and give an insight into what drives electrocatalytic processes at nanostructured gold.[14] In this work we investigate the electrochemical behaviour of gold that is often employed in applied studies in the form of a conventional commercial bulk electrode, as an evaporated thin film, and in the nanostructured form such as well dispersed hierarchical structures and a continuous porous honeycomb network where the latter is an extension of our previous communication.[37] This analysis is done with conventional electrochemical techniques such as dc cyclic voltammetry but also with large amplitude Fourier transformed ac (FT-ac) voltammetry which can effectively discriminate between capacitive and Faradaic processes occurring at an electrode surface.[38,39] We demonstrate that active sites exist on gold in all the forms investigated whose coverage depends on the method of synthesis. Significantly, we demonstrate how these active sites allow for the spontaneous and discrete electroless deposition of metals such as silver, platinum and palladium in the form of nanoparticles on their surfaces.

Experimental

Chemicals

Solutions of $KAuBr_4$, H_2SO_4, NaOH (Ajax Finechem), ethanol (Merck), $AgNO_3$, K_2PtCl_4 (Aldrich), $Ni(NO_3)_2$, $Pd(NO_3)_2$ (BDH) were used as received and made up with deionized water (resistivity of 18.2 MΩ cm) purified by use of a Milli-Q reagent deioniser (Millipore). High purity oxygen (5.0 coregas) was purged into

 This journal is © The Royal Society of Chemistry 2011

View Article Online

the relevant solution for at least 20 minutes, otherwise solutions were degassed with nitrogen for at least 10 minutes.

Published on 28 July 2011. Downloaded by Queensland University of Technology on 20/11/2013 23:06:48.

Electrode materials

Gold and platinum electrodes (BAS) of diameter 1.6 mm were used. Gold thin films were deposited by a Balzers™ electron beam evaporator. The layer composed of 1500Å of Au and 100Å of Ti. The films were deposited sequentially by electron evaporation process onto the bare AT-cut quartz substrates. The purpose of the Ti layer is to assist with the adhesion of the Au layer to the substrate surface. Indium tin oxide (ITO) (Prazisions Glas and Optik GmbH) coated glass with a sheet resistance of 10 Ω sq^{-1} as quoted by the manufacturer was used as the substrate for gold nanomaterial electrodeposition.

Materials characterisation

SEM measurements were performed on a FEI Nova SEM instrument (Nova 200). Prior to SEM imaging, samples were thoroughly rinsed with Milli-Q water and dried under a flow of nitrogen. X-ray diffraction data were obtained with a Bruker AX 8: Discover with General Area Detector Diffraction System (GADDS). X-ray photoelectron spectroscopy (XPS) characterization of samples was done using a Thermo K-Alpha instrument at a pressure better than 1×10^{-9} Torr. The core level binding energies (BEs) were aligned with the adventitious C 1s binding energy of 285 eV.

Electrochemical measurements

Cyclic voltammetric experiments were conducted at (20 ± 2) °C with a CH Instruments (CHI 760C) electrochemical analyser in an electrochemical cell (BAS) that allowed reproducible positioning of the working, reference, and counter electrodes and a nitrogen inlet tube. ITO and e-beam evaporated Au films when used as the working electrode were sonicated and washed in acetone and methanol respectively followed by drying in a stream of nitrogen gas prior to use. The gold or platinum (BAS) electrode was polished with an aqueous 0.3 μm alumina slurry on a polishing cloth (Microcloth, Buehler), sonicated in water and dried with nitrogen. The reference electrode was Ag/AgCl (aqueous 3 M KCl). For electrodeposition experiments an inert graphite rod (3 mm diameter, Johnson Matthey Ultra "F" purity grade) was used as the counter electrode to prevent contamination by any electrolysis products.[40] All electrochemical experiments were commenced after degassing the electrolyte solutions with nitrogen for at least 10 min prior to any measurement.

FT-ac measurements

A description of the FT voltammetric instrumentation used in this study is available elsewhere.[41] Sine waves of frequencies $f = 21.29$ Hz and amplitudes of $\Delta E = 100$ mV were employed as the ac perturbation. DC voltammetric experiments were also carried out with this instrumentation by using a zero amplitude perturbation to compare with results obtained using the CH Instruments potentiostat.

Results and discussion

Electrochemical characterisation of unactivated and activated gold electrodes

Illustrated in Figure 1 is a typical cyclic voltammogram for a polycrystalline commercial gold electrode in 1 M H_2SO_4. It can be seen that there is an extensive double layer region from the beginning of the sweep until the onset of compact monolayer oxide formation (Au_2O_3) at *ca.* 1.20 V. On the reverse sweep this oxide

View Article Online

Published on 28 July 2011. Downloaded by Queensland University of Technology on 20/11/2013 23:06:48.

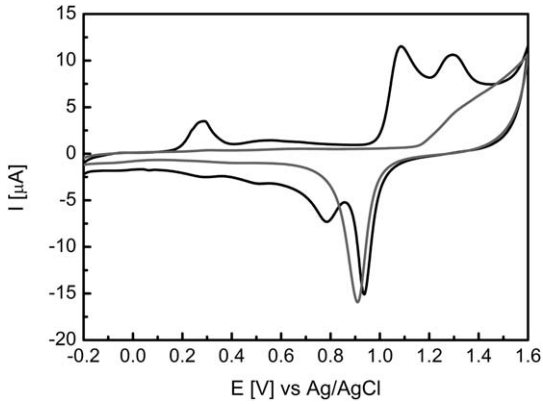

Fig. 1 CVs recorded in 1 M H_2SO_4 at a sweep rate of 100 mV s^{-1} for an untreated polycrystalline gold electrode (grey) and activated by polarisation at −1.5 V for 10 min in 1 M H_2SO_4 (black).

is removed in a sharper reduction process with a peak potential at 0.91 V where the hysteresis observed is due to a place exchange process which occurs during oxide formation.[24] If this electrode is activated by polarisation at a potential where hydrogen gas is evolved from the surface for 10 minutes and transferred to fresh H_2SO_4 solution then distinctly different voltammetry is observed. The double layer region now shows distinct oxidation processes at *ca.* 0.29, 0.55 and 1.08 V. These processes show a degree of reversibility with the associated reduction peaks observed at 0.26, 0.50 and 0.78 V respectively.

It has been postulated by Burke that polarisation of gold in the hydrogen evolution region disrupts the outer layer of the metal through a process akin to hydrogen embrittlement.[42] This creates low co-ordinated gold clusters which are more readily oxidised than the bulk metal which begins at 1.20 V. Recently it has been demonstrated that not only gold[43] but also silver[44] and lead[45] nanoparticles show evidence of size dependent electro-oxidation where the oxidation potential occurs at less positive potentials as the size of the nanoparticles decreases. This may also be the origin of such processes occurring at different potentials in that the cluster size of atoms generated are highly likely to be polydisperse in nature. The possibility of impurities being electrodeposited and subsequently stripped from the surface is discounted as this type of behaviour has also been reported for thermally treated electrodes that have been rapidly quenched under nitrogen[25] and oxygen[9] atmosphere and more recently by gold nanoparticles that have been sonochemically activated[26] where the possibility of depositing metallic impurities is minimal. It also raises the question as to whether calculating the surface area of gold using the charge associated with the reduction of the monolayer oxide as described by Woods[46] and used extensively in this area is valid for such highly active surfaces.

It is interesting to note that a significant number of electrocatalytic reactions occur on gold in acidic medium at discrete electrode potentials which coincide with the potentials at which these active site responses are observed. Illustrated in Figure 2 are three electrocatalytic reactions which occur at different regions within the double layer region of gold. It can be seen that hydrogen peroxide reduction (Figure 2b) begins at *ca.* 0.29 V, hydrazine oxidation (Figure 2c) at *ca.* 0.63 V and hydrogen peroxide oxidation (Figure 2d) at *ca.* 1.00 V which are at the potentials in which the activated gold electrode was shown to be oxidised (Figure 2a). It has been shown previously that several electrocatalytic reactions on gold in acidic solution are grouped at these distinct potentials in which the generation of surface active sites controls the reactions of interest.[21]

 This journal is © The Royal Society of Chemistry 2011

View Article Online

Published on 28 July 2011. Downloaded by Queensland University of Technology on 20/11/2013 23:06:48.

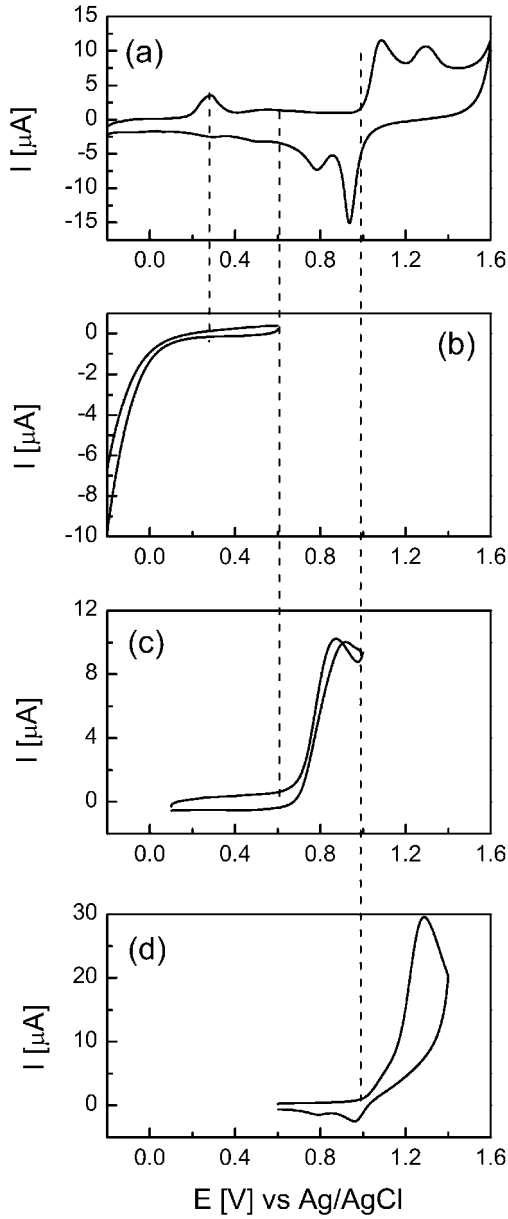

Fig. 2 CVs recorded in 1 M H_2SO_4 for (a) an activated gold electrode at a sweep rate of 100 mV s^{-1} and an unactivated gold electrode in (b) containing 20 mM H_2O_2 at a sweep rate of 20 mV s^{-1}, (c) containing 50 mM N_2H_4 at 50 mV s^{-1} and (d) containing 20 mM H_2O_2 at a sweep rate of 20 mV s^{-1}.

It has been reported that activating a gold surface may enhance electrocatalytic activity by promoting the formation of active sites. However, given that electrocatalytic reactions are mediated by the above mentioned processes at an unmodified gold electrode, suggests that active sites are inherently present on the surface. To investigate this phenomenon a variety of gold surfaces were investigated to see if active sites were indeed present and if their coverage was dependent on the method of fabrication.

Published on 28 July 2011. Downloaded by Queensland University of Technology on 20/11/2013 23:06:48.

Anisotropic microstructures. The electrodeposition of anisotropic gold structures for electrocatalytic and SERS applications has received significant attention. To determine if active site behaviour can be observed by electrochemical methods, "hedgehog" like anisotropic gold structures electrodeposited onto an ITO substrate were investigated. Briefly, gold was electrodeposited from an aqueous 5 mM $KAuBr_4$ solution at a potential of 0.30 V vs Ag/AgCl for 60 s. As shown in Figure S1 this potential is well before the peak maximum observed in the cyclic voltammogram recorded for Au electrodeposition onto ITO.† This value was chosen to prevent growth occurring at a diffusion limited rate and therefore encourage the growth of anisotropic structures, while the time was chosen to avoid the formation of a continuous film. Illustrated in Figure 3 are SEM images of the type of structures that can be formed. They consist of intertwined flat plates to give an overall "hedgehog" type morphology. XRD characterisation (Figure S2) confirmed that this material is polycrystalline in nature without any preferred crystallographic orientation as seen also for the polycrystalline gold electrode (Figure S2).†

CVs were then recorded in 1 M H_2SO_4 and are shown in Figure 4. It can be seen that there are active state responses which are similar to those seen for the gold electrode polarised in the hydrogen evolution region (Figure 1). There are active site oxidation responses at *ca.* 0.28 V, and a broad response centred at 0.78 V. Each of these processes has an associated cathodic counterpart. However, there is an interesting difference between the responses observed over the potential range of 1.0 to 1.6 V. The anisotropic structures are oxidised in one broad process which commences at a potential (*ca.* 1.0 V) below that for regular monolayer oxide formation (1.20 V). On the subsequent reduction sweep two cathodic processes can be observed at *ca.* 0.78 V and 0.52 V as observed for the activated gold electrode but the magnitude of the reduction peak at the lower potential is significantly higher in the case of anisotropic gold. Again this illustrates a difficulty in estimating the surface area of this material based on the electrochemical reduction of a monolayer oxide, as three distinct oxide reduction processes are evident.

Given that there were no obvious differences in the crystallographic nature of the gold nanostructures (Figure S2)† and of the activated gold electrode, the presence of specific gold plane oxidation processes as observed in single crystal studies can be discounted.[16] It also confirms that the responses observed for an electrode activated by cathodic polarisation are not due to the oxidation of sub surface hydrides that may have been formed during the activation process.

Porous honeycomb structures. As demonstrated in a recent publication[37] porous honeycomb gold can be created using a hydrogen bubble templating method in

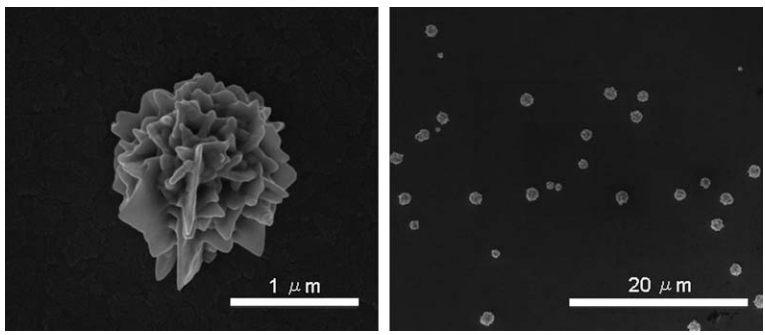

Fig. 3 SEM images of anisotropic gold structures deposited for 60 s at 0.3 V on an ITO substrate.

 This journal is © The Royal Society of Chemistry 2011

View Article Online

Published on 28 July 2011. Downloaded by Queensland University of Technology on 20/11/2013 23:06:48.

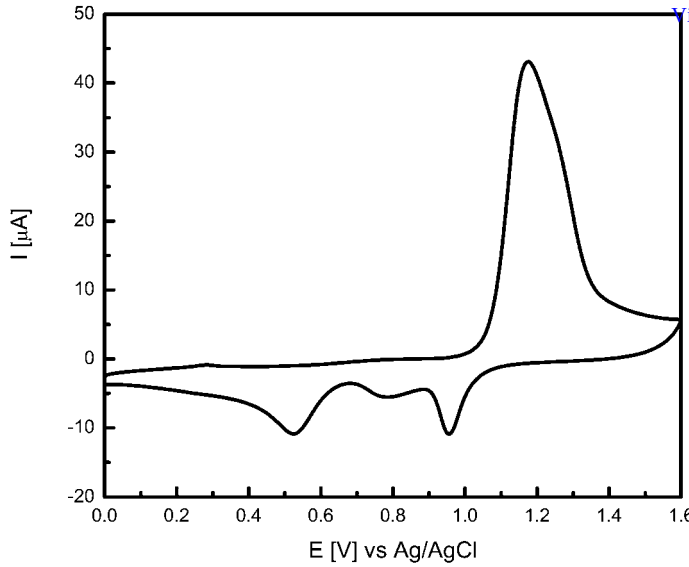

Fig. 4 CV for anisotropic Au structures (as in Figure 3) on ITO in 1 M H_2SO_4 recorded at a sweep rate of 50 mV s^{-1}.

which vigorous hydrogen gas evolution during the course of the electrodeposition process allows metal to be deposited around the evolving hydrogen bubbles to create a highly porous structure. In this case a honeycomb gold film was created from a 0.1 M $KAuBr_4$ + 1.5 M H_2SO_4 solution using a current density of 2 A cm^{-2} for 30 s. A typical SEM image of the type of structure is shown in Figure 5a with the inset showing a higher magnification image demonstrating the highly dendritic nature of the internal wall structure. Given this type of nanostructure and the fact that vigorous hydrogen evolution occurred during the synthesis, which is analogous to the activation method described for creating the type of surface characterised in Figure 1, it is not surprising that significant active site responses are observed in the double layer region. It is interesting to note the responses at potentials below 0.20 V (Figure 5b) which were not observed for the activated gold electrode or the

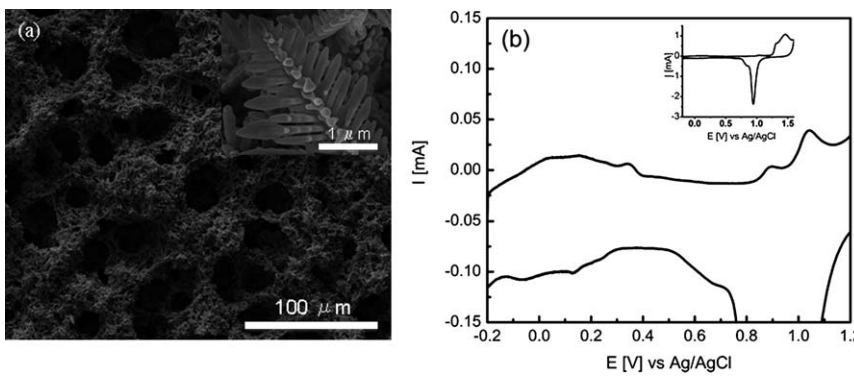

Fig. 5 SEM image showing the honeycomb film formed through the dynamic hydrogen bubble technique (a), where the dendritic nature of the pore walls is seen in the inset image. CV of the honeycomb film recorded at 50 mV s^{-1} in 1 M H_2SO_4 (b), showing a magnified view along with the overall response (inset).

View Article Online

Published on 28 July 2011. Downloaded by Queensland University of Technology on 20/11/2013 23:06:48.

anisotropic gold nanostructures which may be magnified due to the increased surface area of the material. The inset in Figure 5b shows the full CV where the magnitude of the monolayer oxide/reduction processes masks the double layer region responses given the very high surface area of the honeycomb gold.[37] This porous honeycomb material is presented here as the creation of a very active surface is shown to be highly beneficial for the creation of bimetallic systems which is discussed later through a simple electroless deposition route which is driven by the presence of active sites on the surface.

Evaporated thin films. The generation of nanostructured gold is interesting from both a fundamental and application point of view, however, nanostructured or rough high surface area materials are not always required for every application. Gold is routinely used in the microelectronics industry and as a decorative material where smooth shiny deposits are preferred. Therefore, the electrochemical behaviour of evaporated thin films of gold was also investigated. Illustrated in Figure 6a is a SEM image of a 150 nm thick film of gold. It can be seen that the individual grains are *ca.* 50 nm in diameter with the presence of a significant amount of grain boundaries. The CV behaviour of this thin film in 1 M H_2SO_4 shows that the double layer region is not completely free of active site behaviour (Figure 6b). There is a broad anodic feature centred at 0.53 V and the onset of monolayer oxide formation occurs at *ca.* 1.00 V as seen in the case of an activated gold electrode and the anisotropic gold nanostructures. Therefore, this data suggests that even relatively smooth evaporated films of gold have an inherent activity which may dictate the electrocatalytic performance of gold.

Electrochemical characterization of porous honeycomb gold using large amplitude FT-ac voltammetry

The possibility that the responses observed in the double layer are purely due to capacitive effects associated with specific anion adsorption can also be ruled out. Recently, Bond *et al.* have developed the large amplitude Fourier Transformed ac voltammetry technique which offers the unique advantage of being able to effectively discriminate between capacitive and Faradaic processes in the higher ac harmonic responses occurring at the electrode surface.[39,47–50] Also, analysis of the shape of the higher harmonic responses allows the reversible nature of the Faradaic process to be investigated. Illustrated in Figure 7 are the dc and fundamental to fourth harmonic ac responses recorded for honeycomb porous gold in 1 M H_2SO_4. The data is split into the forward (a1 to e1) and reverse (a2 to e2) sweeps for clarity of presentation.

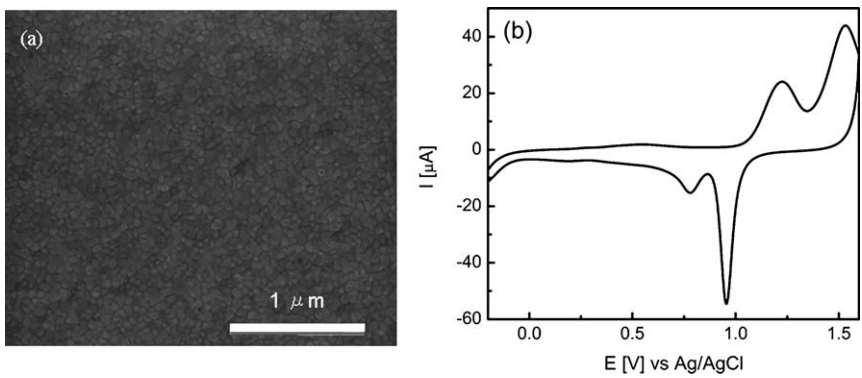

Fig. 6 An SEM image of an evaporated gold film (a) and a CV of the gold film recorded at 50 mV s^{-1} in 1 M H_2SO_4 (b).

 This journal is © The Royal Society of Chemistry 2011

View Article Online

Published on 28 July 2011. Downloaded by Queensland University of Technology on 20/11/2013 23:06:48.

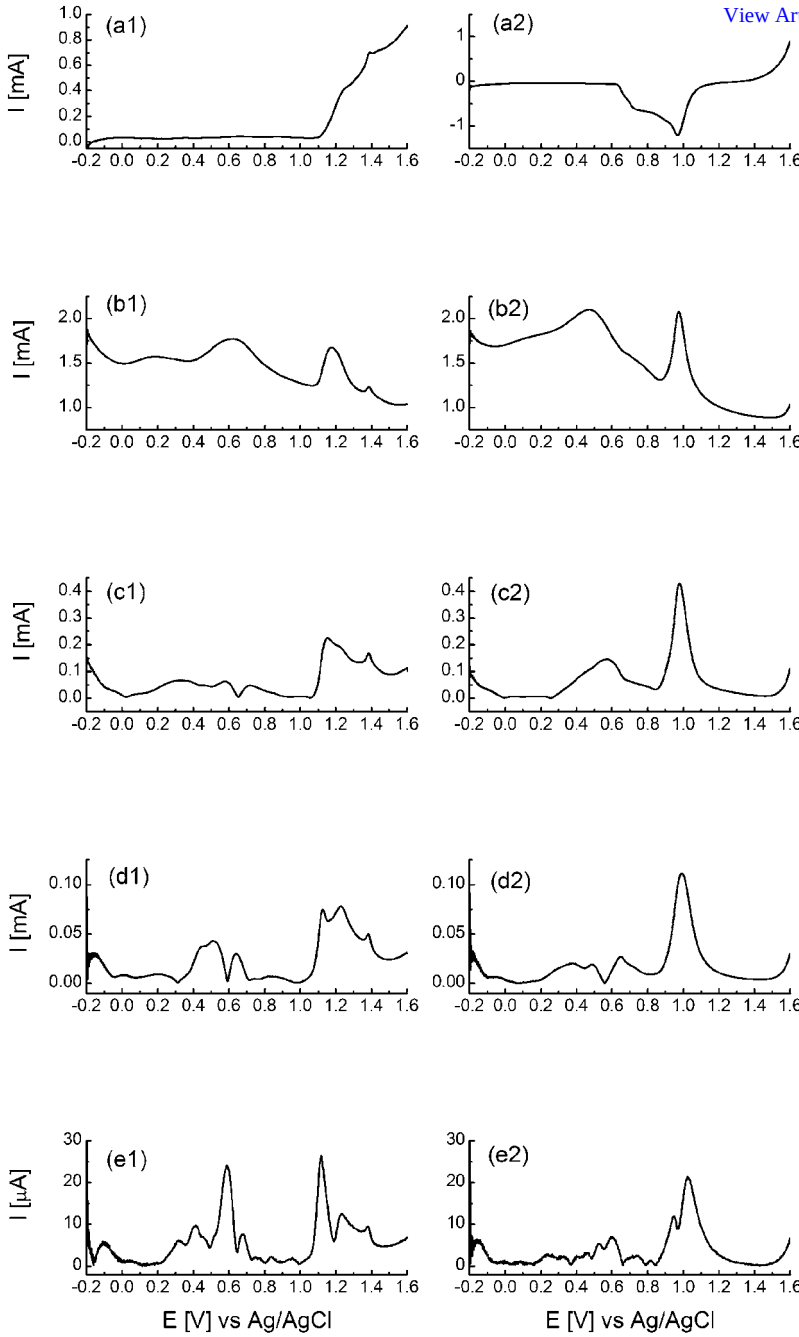

Fig. 7 Large amplitude Fourier transformed ac cyclic voltammograms obtained for the dc (a) and fundamental to fourth harmonics (b–e) for honeycomb porous gold in 1 M H_2SO_4. Conditions employed: $f = 21.16$ Hz, $\Delta E = 100$ mV and $\nu = 67.06$ mV s^{-1}.

In the dc component (a1) very little evidence is seen for active site behaviour as the response is masked by the magnitude of the monolayer oxide formation response as discussed previously. However, from analysis of the fundamental (b1), second (c1), third (d1) and fourth (e1) ac harmonics it can be seen that distinct processes begin to

View Article Online

Published on 28 July 2011. Downloaded by Queensland University of Technology on 20/11/2013 23:06:48.

emerge at −0.10, 0.38, 0.60 and 1.12 V which coincide with that observed for the activated gold electrode and the evaporated thin film. In particular, in the fourth harmonic ac response the influence from background capacitive current can be assumed to be negligible which therefore indicates that significant Faradaic processes occur within the double layer region of gold. From analysis of the peak shape and the magnitude of the associated responses on the reverse sweep (a2–e2) it shows that each response is most likely quasi-reversible in nature as discussed recently by Bond.[51] The decrease in the magnitude of the responses in the reverse sweep may be related to the stability of the oxidation product of gold in this environment. It can also be seen that there is a response at the beginning of the monolayer oxide formation process at *ca.* 1.2 V which can be associated with electron transfer between gold and hydroxide ions before the place exchange reaction begins to form the compact Au_2O_3 oxide. Therefore, this suggests that the type of responses observed here over the potential range of −0.2 to 1.2 V using dc cyclic voltammetry are most likely to be Faradaic in nature. This was confirmed for both the anisotropic gold nanostructures on ITO and the evaporated thin film where FT-ac voltammograms for the dc and fundamental to fourth ac harmonics are shown in Figures S3 and S4 respectively.

It has been suggested in the literature that the oxidation of active sites on gold results in the formation of an extremely low coverage of β-hydrous oxide material on the surface where Burke[24] has postulated that these incipient oxides may be formulated as $[Au_2(OH)_9]^{3-}{}_{ads}$. In a recent paper by Bard *et al.* the surface interrogation mode of scanning electrochemical microscopy technique was used to detect these incipient oxides by reducing them using a locally generated flux of reductant from a microelectrode tip which indicated that the coverage can be as great as 0.2 of a monolayer.[52] Given the nature of this oxidation product in acidic medium it is most likely to be unstable which would account for the decreased magnitude of the response in the higher harmonics in the reverse sweep.

Therefore, the porous honeycomb gold was also characterized by FT-ac voltammetry in 1 M NaOH to observe the stabilization of a $[Au_2(OH)_9]^{3-}{}_{ads}$ species under conditions employing a high concentration of OH^- ions (Figure 8). It can be seen in the higher harmonics (d1 and e1 in particular) that three distinct processes can be observed at −0.80, −0.15 and 0.20 V which all occur before the onset of compact monolayer oxide formation. The shape of the responses in fourth ac harmonic are better defined than in the case of the same material in acid medium (Figure 7e1) and resemble those achieved for a surface confined redox process with fast electron transfer.[39,48] The process at −0.20 V seems particularly reversible in nature given the comparable magnitude achieved in both the forward (e1) and reverse (e2) sweeps. Significantly, well defined processes in the higher ac harmonics were also observed in the case of a thin film of gold as shown in Figure S5.† The FT-ac voltammetry technique was not applied to the case of anisotropic nanostructures on ITO given the reported instability of ITO in alkaline medium at low potential values and current densities of the order of −2 mA cm^{-2} which results in the reduction of Sn^{IV} to Sn^{II}.[53] Even though the timescale of a CV experiment is relatively short this complication was avoided given the extremely sensitive nature of the FT-ac technique to detect electron transfer processes. It should be noted that this Sn^{IV} to Sn^{II} process is avoided in acidic medium in the potential region of study and that FT-ac voltammograms recorded for ITO only did not shown any significant response above the noise level of the instrument.

Electrocatalytic reactions at porous honeycomb gold

Illustrated in Figure 9a is the electrooxidation of hydrogen peroxide at porous honeycomb gold in 1 M H_2SO_4 solution. It can be seen that the onset potential is at *ca.* 0.66 V which is 0.34 V less positive than that observed on the polycrystalline electrode (Figure 2d). This shift in onset potential is generally regarded as being an

 This journal is © The Royal Society of Chemistry 2011

View Article Online

Published on 28 July 2011. Downloaded by Queensland University of Technology on 20/11/2013 23:06:48.

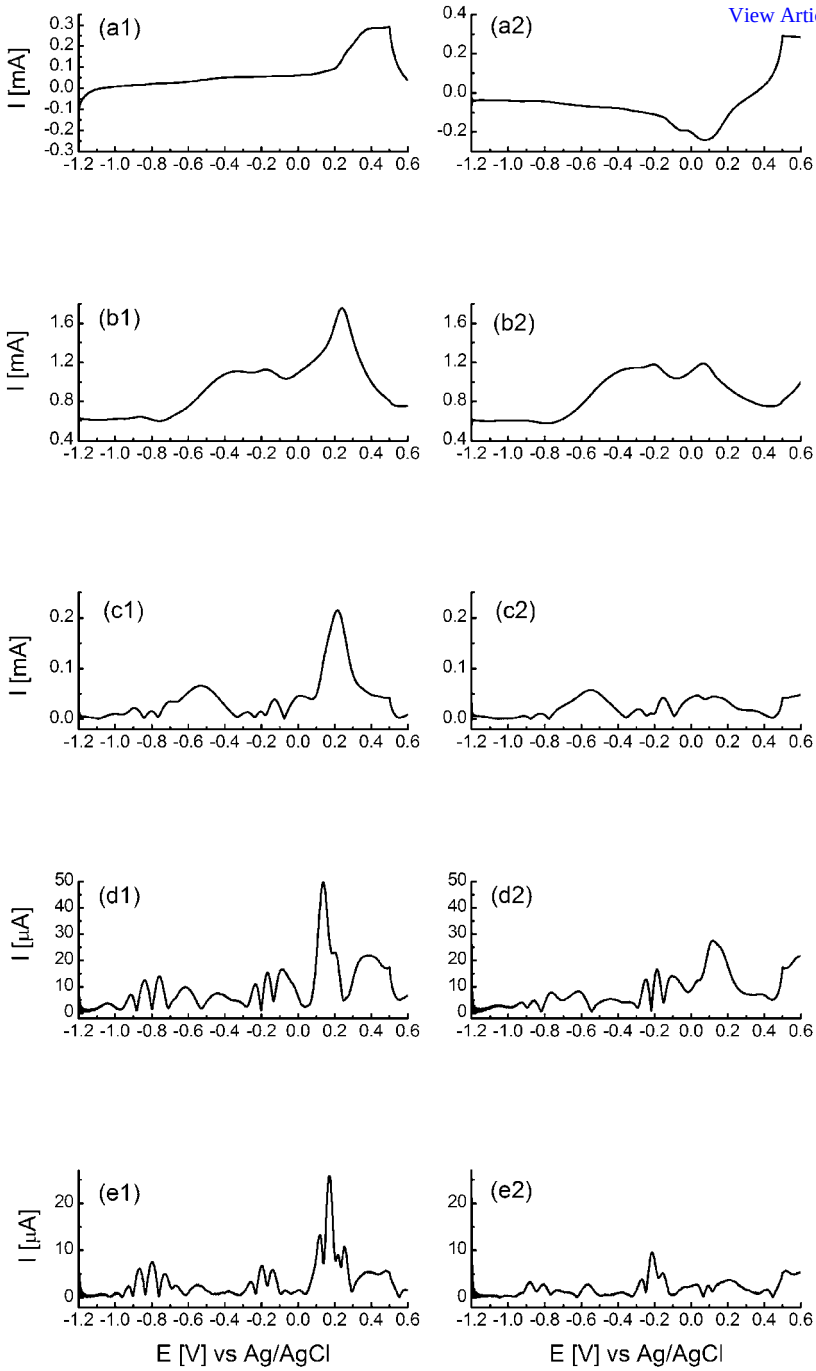

Fig. 8 Large amplitude Fourier transformed ac cyclic voltammograms obtained for the dc (a) and fundamental to fourth harmonics (b–e) for honeycomb porous gold in 1 M NaOH. Conditions employed: $f = 21.16$ Hz, $\Delta E = 100$ mV and $\nu = 63.33$ mV s^{-1}.

indication of an electrocatalytic effect. It is interesting to note however that the reaction commences at a potential where an active state response was recorded with the FT-ac voltammetry technique at 0.60 V (Figure 7). This suggests that the presence of

View Article Online

Published on 28 July 2011. Downloaded by Queensland University of Technology on 20/11/2013 23:06:48.

a significant active state response at lower potential on the nanostructured porous gold is more favourable for hydrogen peroxide oxidation, by possibly changing the thermodynamics of the process from that observed at the more positive active site response at *ca.* 1.00 V. The electroreduction of dissolved oxygen under acidic conditions is illustrated in Figure 9b. The onset potential occurs at *ca.* 0.22 V with a further increase in current detected at *ca.* −0.02 V. Significantly, active site responses are recorded close to these potentials on porous gold in 1 M H_2SO_4 only (Figure 7).

A similar type of behaviour was recorded at the porous honeycomb gold for electrocatalytic reactions carried out under alkaline conditions in that the reactions occurred at potentials where active sites responses were observed. Illustrated in Figure 10a is the electro-oxidation of ethanol in 1 M NaOH. It can be seen that the onset potential is *ca.* −0.38 V which is just prior to the active site response recorded in 1 M NaOH only (Figure 8). The electroreduction of oxygen (Figure 10b) commences at *ca.* 0.00 V with a further increase observed at −0.16 V where the latter is at a potential of a significant active site response (Figure 8).

In all the electrocatalytic reactions investigated it appears that each reaction is being mediated at discrete potentials which coincide with the observation of oxidation responses of gold in the double layer region. Therefore it seems that the incipient hydrous oxide adatom mediator (IHOAM) model of electrocatalysis postulated by Burke for polycrystalline gold wire electrodes[14,25,54] is also applicable to nanostructured gold. This model postulates that the incipient oxide species, generated upon the oxidation of active surface atoms of gold, can be a mediator for oxidation of a dissolved reductant, whereas the mediator for reduction reactions can be the bare surface atoms themselves. This surface confined mediator approach to electrocatalysis does not account for activated chemisorption, however the possibility of the latter cannot be completely discounted.[21,55]

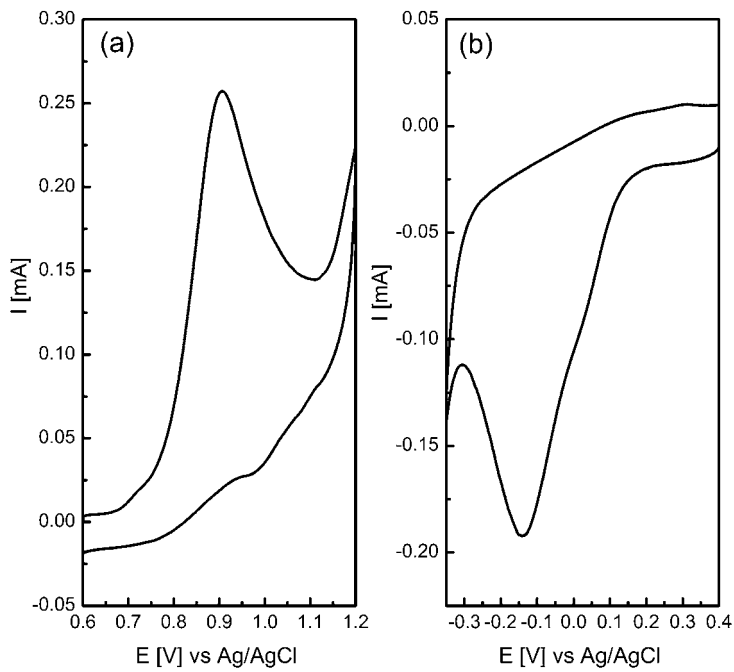

Fig. 9 CVs recorded at porous honeycomb gold at a sweep rate of 20 mV s^{-1} in 1 M H_2SO_4 solution containing (a) 20 mM H_2O_2 and (b) saturated with oxygen.

 This journal is © The Royal Society of Chemistry 2011

View Article Online

Published on 28 July 2011. Downloaded by Queensland University of Technology on 20/11/2013 23:06:48.

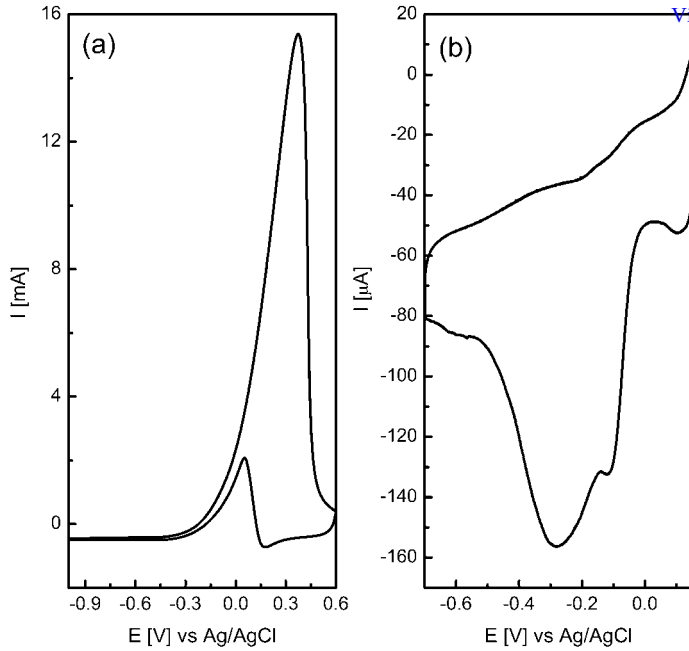

Fig. 10 CVs recorded at porous honeycomb gold in 1 M NaOH solution containing (a) 1 M ethanol obtained at a sweep rate of 50 mV s^{-1} and (b) saturated with oxygen obtained at a sweep rate of 20 mV s^{-1}.

Decoration of active gold with metal nanoparticles

A recent method to create bimetallic nanoparticles and surfaces is the galvanic replacement method which has resulted in an array of porous, hollow, dendritic and high surface area materials with compositions such as Ag/Au, Ag/Pt, Co/Pt, and Fe/Au.[56–61] When this approach is used, the thermodynamic driving force for the reaction is the difference in the standard electrode reduction potentials between the sacrificial metal/metal ion couple and the solution based metal/metal ion couple. For the case of gold its decoration using this approach is problematic given the high standard reduction potential of the Au^{3+}/Au couple (1.50 V vs SHE). Even if a chloride media was employed the standard reduction potential of $AuCl_4^-$/Au is still high at a value of 1.002 V vs SHE). In this work the active state responses observed in the double layer region of gold are assumed to be due to the more facile oxidation of gold in an active state than the bulk material. Therefore if active gold is more readily oxidised then it should allow for spontaneous electroless deposition of metal species to occur that have a standard reduction potential greater than the potential at which these active sites are oxidised. A porous honeycomb gold sample was then immersed in separate 1 mM aqueous solutions of $Ni(NO_3)_2$, $AgNO_3$, $Pd(NO_3)_2$ and K_2PtCl_4 where the standard reduction potentials of Ni^{2+}/Ni, Ag^+/Ag, Pd^{2+}/Pd and $PtCl_4^{2-}$/Pt are −0.257 V, 0.799, 0.915 and 0.758 V vs SHE respectively. It can be seen that these standard reduction potentials are significantly lower than that for the Au^{3+}/Au couple and therefore the spontaneous replacement of gold is not expected. However, upon immersion of honeycomb porous gold in $AgNO_3$ and $Pd(NO_3)_2$ significant decoration of the surface with nanoparticles can be observed (Figure 11).

For the case of silver, surface decoration was confirmed by XPS (Figure S6),† and CV analysis and SEM images are shown in Figures 11a and b. It can be seen that the dendritic nanostructures are well decorated with silver nanoparticles (Figure 11a).

View Article Online

The nanoparticles are quasi spherical in nature with particle sizes ranging between 15 to 40 nm (Figure 11b). It can also be seen that the silver nanoparticles grow outwards from the surface of gold, in particular at the tip of the dendrites, showing that this process is driven from the surface of the material and that nanoparticles are not formed in solution. It should also be noted that the overall macroporous morphology of the honeycomb material was preserved (Figure S7).† After immersion of porous gold in $Pd(NO_3)_2$ the presence of Pd nanoparticles can be observed which was confirmed by XPS (Figure S6) and CV analysis. In this case however, growth appears to be limited to the tips, edges and protruding backbone of each dendrite (Figure 11c). Also, it can be seen that the size of the nanoparticles are much smaller compared to the case of silver decoration with diameters ranging from 5 to 15 nm (Figure 11d). From the CV analysis of porous gold in aqueous solution (Figure 5b) there are a significant number of oxidation responses at potential values lower than the standard reduction potentials of the Ag^+/Ag and Pd^{2+}/Pd couples. This would provide the required driving force for spontaneous metal

Published on 28 July 2011. Downloaded by Queensland University of Technology on 20/11/2013 23:06:48.

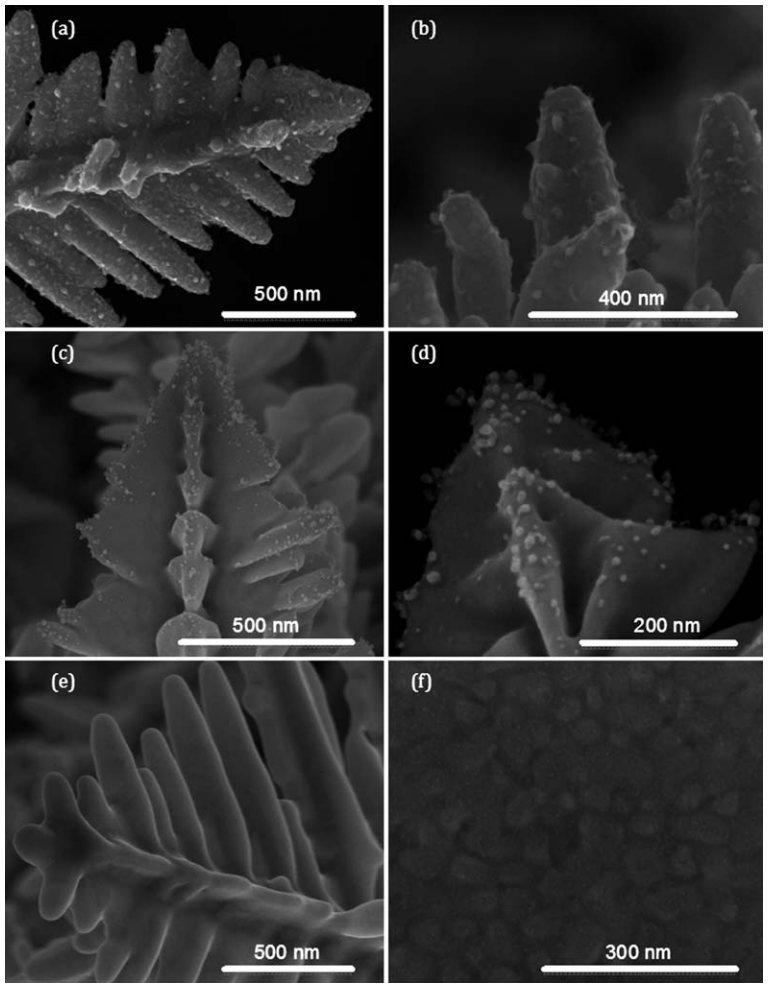

Fig. 11 SEM images showing the decoration of honeycomb structures after 5 min immersion in 1 mM solutions of $AgNO_3$ (a, b) $Pd(NO_3)_2$ (c, d) and K_2PtCl_6 (e) along with an evaporated gold substrate after 5 min immersion in 1 mM $Pd(NO_3)_2$.

 This journal is © The Royal Society of Chemistry 2011

View Article Online

Published on 28 July 2011. Downloaded by Queensland University of Technology on 20/11/2013 23:06:48.

deposition to occur whereby the facile oxidation of active gold provides the electrons for reduction of the Ag^+ and Pd^{2+} ions. To provide further evidence for this mechanism it was noted that when $Ni(NO_3)_2$ solution was employed there was no observation of surface decoration with Ni nanoparticles by SEM or that could be detected with XPS and CV analysis. The Ni^{2+}/Ni couple has a standard reduction potential of −0.257 V vs SHE which is in the hydrogen evolution region on gold where no active site responses can be observed and it is highly unlikely that gold could be oxidised at potentials lower than this. It should be noted that the synthesis of the porous gold material requires vigorous hydrogen evolution and so the possibility of adsorbed hydrogen acting as a reductant was investigated. This mechanism can be discounted as an evaporated gold film immersed in $Pd(NO_3)_2$ showed the presence of palladium nanoparticles as illustrated in Figure 11f. The particles have a diameter of less than 10 nm as in the case of porous gold but interestingly do not show preference for decoration of the grain boundaries suggesting that active sites are present all over the surface.

Interestingly, when a 1 mM solution of K_2PtCl_4 was used, surface decoration with Pt nanoparticles could not be observed by SEM (Figure 11e). However, XPS analysis confirmed the presence of metallic platinum even though the signal was quite weak (Figure S6c).† A CV was obtained in 1 M H_2SO_4 (Figure 12a) and it can be seen that there is a characteristic hydrogen adsorption/desorption region over a potential range of −0.22 to −0.14 V associated with metallic platinum. When the hydrogen evolution reaction is carried out a significant shift in onset potential and magnitude of the response is observed compared to the unmodified porous gold which further confirms the presence of platinum (Figure S8).† A continuous thin layer of platinum on the surface is discounted as distinct voltammetry from gold can be seen. Indeed the surface coverage with platinum appears to be quite low when the CV responses associated with platinum and gold are compared which explains the weak XPS signal. Taking the electrochemically active surface area of both gold and platinum indicates a 5% coverage of the surface with platinum. The surface area of gold was calculated using the charge associated with the monolayer oxide reduction peak[46] at 0.93 V and a value of 400 μC cm^{-2}. The contribution from the reduction of incipient oxides formed on the forward sweep at potentials lower than 0.93 V on active gold is not taken into account here. It should be noted that these responses are significantly less than the monolayer oxide reduction peak unlike the case of anisotropic structures on gold which demonstrated three significant reduction peaks. The surface area of platinum was calculated using the charge associated with the desorption of hydrogen[62] and a value of 210 μC cm^{-2}. The calculated metal coverage is slightly higher than the *ca.* 1% of an unactivated surface that has been estimated by Burke to be active for electrocatalytic reactions. This is most likely due to the method of synthesis which introduces a higher amount of metastable surface sites. This percentage coverage with platinum suggests that perhaps extremely small nanoparticles are produced that cannot be observed at the resolution achievable by the field emission SEM instrument used in this study. A high resolution TEM study will be undertaken to confirm this hypothesis. It can also be seen that the double layer region is now absent of active site responses from 0.20 to 1.10 V (inset Figure 12a) where significant responses were observed for the unmodified surface (Figure 5b) illustrating the role of these sites in the electroless deposition process.

The CV responses for the Au/Pd and Au/Ag systems are shown in Figures 12b and c respectively. For Au/Pd a characteristic hydrogen adsorption/desorption region can be observed, indicating the presence of metallic palladium, and similarly metallic platinum is observed in the case of Au/Pt (Figure 12a and inset), where the former is shifted to more negative potentials compared to the latter. There is some evidence of active site behaviour, with a process observed at 0.52 V, which suggests that not all active sites are decorated with palladium. The Au/Ag material was characterised by CV in 1 M NaOH to avoid the electrodissolution of Ag that occurs in acidic media.

View Article Online

Published on 28 July 2011. Downloaded by Queensland University of Technology on 20/11/2013 23:06:48.

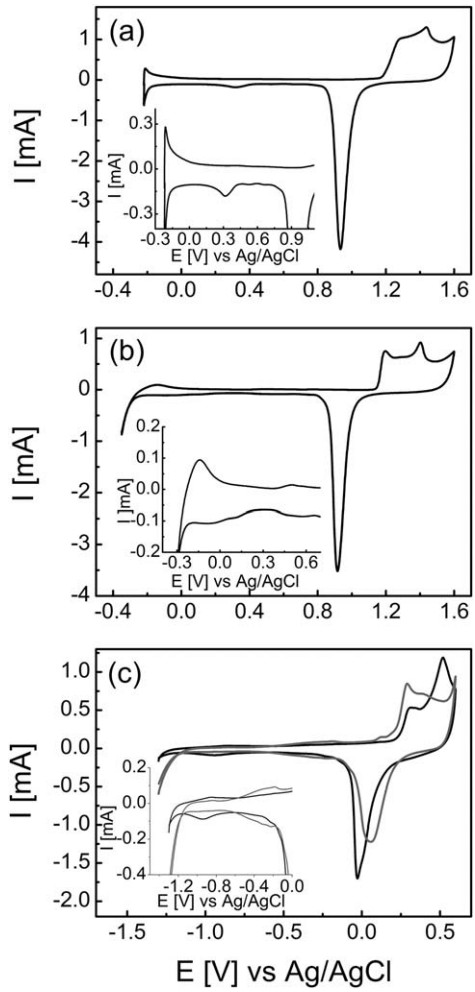

Fig. 12 CVs recorded at porous honeycomb gold at a sweep rate of 50 mV s^{-1} decorated with (a) platinum, (b) palladium and (c) silver. The electrolyte employed was 1 M H_2SO_4 (a and b) and 1 M NaOH (c) where the CV is also shown for porous gold only (grey).

It can be seen in Figure 12c that a distinct oxidation process at 0.50 V can be observed which is indicative of oxide formation on silver.[63] On the reverse sweep the large cathodic peak centred at −0.03 V is at a slightly lower potential than the unmodified gold surface due to the added contribution from silver oxide reduction which occurs over a similar potential region.[63] It can also be seen that the increase in current observed from −1.0 to −1.2 V on gold only, due to the evolution of hydrogen, is nearly completely absent once the surface is decorated with silver (inset of Figure 12c). Given that the surface is only partly decorated with silver nanoparticles (Figure 11a) and that there is a significant amount of gold still available for the hydrogen evolution reaction suggests that the silver nanoparticles block the active sites on gold which are responsible for this electrocatalytic reaction.

This method of chemically interrogating the surface of gold is in a way analogous to the recent work of Scholz who elegantly demonstrated that active sites on gold are attacked by Fenton's reagent where asperities, assumed to be the origin of the active site, are dissolved through a reaction with hydroxyl radicals.[27] The activity of a gold

 This journal is © The Royal Society of Chemistry 2011

View Article Online

Published on 28 July 2011. Downloaded by Queensland University of Technology on 20/11/2013 23:06:48.

electrode was shown to decrease with exposure time to Fenton's reagent for the reduction of dissolved oxygen and also the hydrogen evolution reaction. We believe that our approach of decorating gold with other metals in fact indicates the location of regions with higher densities of active sites on gold surfaces. In the case of the evaporated gold film the coverage was quite uniform, however, the honeycomb porous gold showed highly preferred deposition at the tips and edges of the dendritic nanostructures within the internal wall structure, in particular when palladium was used. The extent of coverage and size of nanoparticles may also be indicative of the reactive nature of the active site in question as the electroless deposition process will be governed by both thermodynamic and kinetic effects. It is also a facile route for the creation of bimetallic surfaces which have received a lot of interest as electrocatalysts due to beneficial synergistic effects that can enhance both the current response and prolong the use of the catalyst by negating poisoning effects with carbonaceous species.[64–67] Recent work has focused on biofuels such as ethanol as a fuel source, but its electro-oxidation is difficult due to significant poisoning of

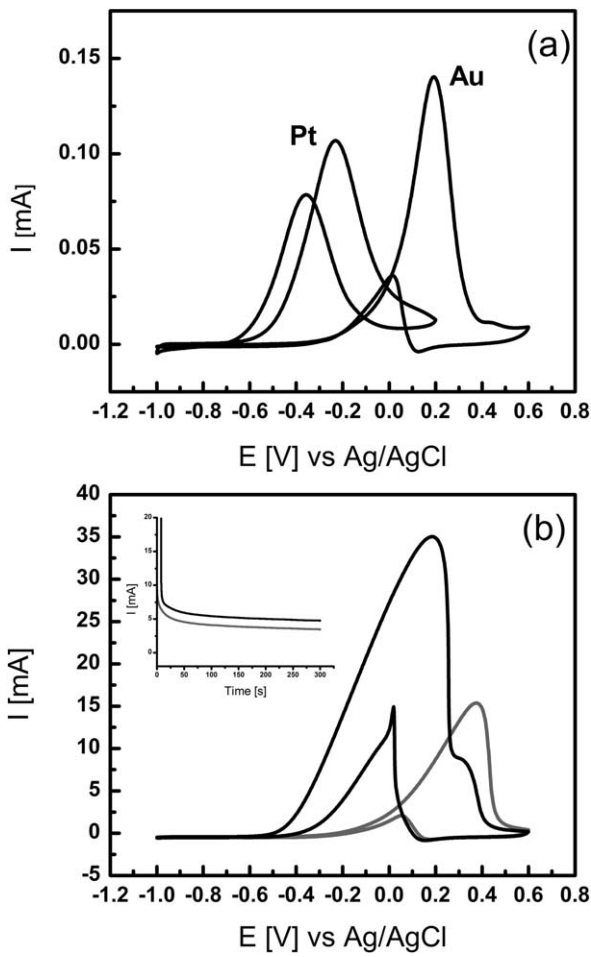

Fig. 13 CVs recorded at a sweep rate of 50 mV s^{-1} in 1 M NaOH containing 1 M ethanol at (a) Pt and Au electrodes and (b) porous gold (grey) and porous gold decorated with platinum (black). The inset shows the current time response when the potential of the relevant electrode was held at 0.18 V.

View Article Online

Published on 28 July 2011. Downloaded by Queensland University of Technology on 20/11/2013 23:06:48.

the electrocatalyst surface.[65] It has been identified that the Au/Pt system is particularly effective in destabilizing adsorbed poisons such as CO by a bi-functional mechanism.[64,65]

The electrocatalytic performance of the bimetallic Au/Pt system was then evaluated for ethanol oxidation in 1 M NaOH which shows significantly different behaviour at gold and platinum electrodes and therefore allows for any synergistic effects of a Au/Pt electrode to be investigated. For a platinum electrode the oxidation of ethanol commences on the positive sweep at −0.60 V and reaches a maximum (I_f) at −0.23 V (Figure 13a). On the negative sweep an oxidation peak is also observed (I_b) which is due to the oxidation of poisoning carbonaceous species, most likely adsorbed CO_{ads}, formed during the positive sweep. It is established that the ethanol oxidation reaction proceeds through the formation of extensive poisoning species such as CO_{ads} on the Pt group of metals. The I_f/I_b ratio observed for Pt is 1.37 and is often used to compare the tolerance of metallic catalysts to poisoning.[68] The electro-oxidation of ethanol on a gold electrode occurs at more positive potentials, demonstrating that it is a less effective catalyst than platinum for this particular reaction. A CV for the oxidation of ethanol on honeycomb porous gold is shown in Figure 13b. The onset for the reaction occurs at *ca.* −0.25 V which is again at a potential where the oxidation of an active site was observed in 1 M NaOH only (Figure 8). The current reaches a maximum at 0.37 V after which it decays due to the formation of the unreactive compact monolayer oxide. On the negative sweep re-oxidation of ethanol commences on gold resulting in a peak at 0.061 V once this oxide has been removed. Upon decoration with Pt a significant increase in electrocatalytic activity is observed. The onset potential is shifted negatively by 0.28 V to −0.53 V with also a significant increase in the magnitude of the current which can be attributed to the higher reactivity of platinum. A minor shoulder at 0.31 V is observed which is attributed to ethanol oxidation on gold only. It is known that platinum is extremely active for the electro-oxidation of ethanol in alkaline conditions but often suffers from severe poisoning effects as seen by the I_f/I_b ratio of 1.37 at the platinum electrode. However, for the porous Au/Pt system a I_f/I_b ratio of 2.30 was attained indicating a much improved tolerance to poisoning. Therefore the stability of the Au and Au/Pt materials were compared by monitoring the current response at a constant potential of 0.18 V. In the inset of Figure 13b it can be seen that the magnitude of the current passed for the Au/Pt material always exceeds that of the Au only material and suggests that the enhanced activity of decorative platinum is maintained and that severe poisoning is alleviated. This is in agreement with studies carried out on the Au/Pt and Pd/Pt systems where the presence of Au and Pd allowed more facile adsorption of hydroxyl anions which inhibited the formation of CO_{ads} and resulted in significantly better electrocatalytic activity than that of unmodified Pt.[65,68] The reduction of oxygen under acidic conditions (Figure S9) was also investigated for the Au/Pt and Au/Pd materials which in both cases showed a shift to less negative potentials indicating increased activity in the order Au/Pt > Au/Pd > Au due to the enhanced activity of platinum and palladium nanoparticles over gold.

Conclusions

In this work it was demonstrated that active sites on gold can be detected by electrochemical methods such as dc and FT-ac voltammetry which result in significant pre-monolayer oxide peaks in the double layer region of gold. These transitions are assumed to be Faradaic in nature given the prominent responses observed in the higher ac harmonics that effectively discriminates capacitive and Faradaic processes. It is also suggested that active sites are not only present on severely activated gold electrodes but also on electrodeposited nanostructured gold and even evaporated thin films. The electrocatalytic behaviour of gold was investigated and several reactions were found to proceed at a potential where distinct active site oxidation

 This journal is © The Royal Society of Chemistry 2011

View Article Online

processes were observed in the absence of the analyte under study. This is in agreement with the IHOAM model of electrocatalysis which was previously studied at planar polycrystalline gold electrodes. Significantly, it was found that advantage could be taken of the more facile oxidation of gold in an active state whereby the surface could be decorated with platinum, palladium and silver which is thermodynamically forbidden at bulk fully lattice stabilised gold. This method allows for the formation of interesting bimetallic surfaces such as Au/Pt which was shown to be particularly beneficial for the ethanol oxidation reaction under alkaline conditions. It is also speculated that this type of surface decoration may indicate regions of high density of active sites on surfaces and may be applicable to many other metals and interesting applications.

Published on 28 July 2011. Downloaded by Queensland University of Technology on 20/11/2013 23:06:48.

Acknowledgements

The authors acknowledge Prof. A. M. Bond and Dr. C.-Y. Lee for the provision of instrumentation and assistance with large amplitude FT-ac experiments. Financial support from the Australian Research Council is also gratefully acknowledged.

References

1 M. Haruta, N. Yamada, T. Kobayashi and S. Iijima, *J. Catal.*, 1989, **115**, 301.
2 J. Zeng, Q. Zhang, J. Chen and Y. Xia, *Nano Lett.*, 2010, **10**, 30.
3 T. A. Baker, X. Liu and C. M. Friend, *Phys. Chem. Chem. Phys.*, 2011, **13**, 34.
4 A. Wittstock, J. Biener and M. Baumer, *Phys. Chem. Chem. Phys.*, 2010, **12**, 12919.
5 G. J. Hutchings, *Catal. Today*, 2005, **100**, 55.
6 P. A. Sermon, G. C. Bond and P. B. Wells, *J. Chem. Soc., Faraday Trans. 1*, 1979, **75**, 385.
7 Y. Li, H. J. Schluesener and S. Xu, *Gold Bull.*, 2010, **43**, 29.
8 J. M. Pingarron, P. Yanez-Sedeno and A. Gonzalez-Cortes, *Electrochim. Acta*, 2008, **53**, 5848.
9 J. H. Shim, J. Kim, C. Lee and Y. Lee, *J. Phys. Chem. C*, 2011, **115**, 305.
10 W. Chen and S. Chen, *Angew. Chem., Int. Ed.*, 2009, **48**, 4386.
11 J. Hernandez, J. Solla-Gullon, E. Herrero, A. Aldaz and J. M. Feliu, *J. Phys. Chem. C*, 2007, **111**, 14078.
12 M. S. El-Deab, T. Sotomura and T. Ohsaka, *Electrochim. Acta*, 2006, **52**, 1792.
13 Z. Borkowska, A. Tymosiak-Zielinska and G. Shul, *Electrochim. Acta*, 2004, **49**, 1209.
14 L. D. Burke, *Gold Bull.*, 2004, **37**, 125.
15 Y. Chen, W. Schuhmann and A. W. Hassel, *Electrochem. Commun.*, 2009, **11**, 2036.
16 R. R. Adzic, S. Strbac and N. Anastasijevic, *Mater. Chem. Phys.*, 1989, **22**, 349.
17 X. Han, D. Wang, J. Huang, D. Liu and T. You, *J. Colloid Interface Sci.*, 2011, **354**, 577.
18 D. H. Nagaraju and V. Lakshminarayanan, *J. Phys. Chem. C*, 2009, **113**, 14922.
19 B. K. Jena and C. R. Raj, *J. Phys. Chem. C*, 2007, **111**, 15146.
20 J. Hernandez, J. Solla-Gullon, E. Herrero, A. Aldaz and J. M. Feliu, *Electrochim. Acta*, 2006, **52**, 1662.
21 L. D. Burke and P. F. Nugent, *Gold Bull.*, 1998, **31**, 39.
22 L. D. Burke and A. P. O'Mullane, *J. Solid State Electrochem.*, 2000, **4**, 285.
23 V. Díaz, S. Real, E. Téliz, C. F. Zinola and M. E. Martins, *Int. J. Hydrogen Energy*, 2009, **34**, 3519.
24 L. D. Burke and P. F. Nugent, *Gold Bull.*, 1997, **30**, 43.
25 L. D. Burke, L. M. Hurley, V. E. Lodge and M. B. Mooney, *J. Solid State Electrochem.*, 2001, **5**, 250.
26 Y.-H. Lee, G. Kim, M. Joe, J.-H. Jang, J. Kim, K.-R. Lee and Y.-U. Kwon, *Chem. Commun.*, 2010, **46**, 5656.
27 A. M. Nowicka, U. Hasse, G. Sievers, M. Donten, Z. Stojek, S. Fletcher and F. Scholz, *Angew. Chem., Int. Ed.*, 2010, **49**, 3006.
28 S. Guo, L. Wang and E. Wang, *Chem. Commun.*, 2007, 3163.
29 B. Plowman, S. J. Ippolito, V. Bansal, Y. M. Sabri, A. P. O'Mullane and S. K. Bhargava, *Chem. Commun.*, 2009, 5039.
30 F. Gao, M. S. El-Deab and T. Ohsaka, *Indian J. Chem., A.*, 2005, **44A**, 932.
31 Y. Tian, H. Liu, G. Zhao and T. Tatsuma, *J. Phys. Chem. B*, 2006, **110**, 23478.
32 L. Komsiyska and G. Staikov, *Electrochim. Acta*, 2008, **54**, 168.
33 W. Ye, J. Yan, Q. Ye and F. Zhou, *J. Phys. Chem. C*, 2010, **114**, 15617.
34 J. F. Hicks, D. T. Miles and R. W. Murray, *J. Am. Chem. Soc.*, 2002, **124**, 13322.

View Article Online

Published on 28 July 2011. Downloaded by Queensland University of Technology on 20/11/2013 23:06:48.

35 R. W. Murray, *Chem. Rev.*, 2008, **108**, 2688.
36 R. Sardar, A. M. Funston, P. Mulvaney and R. W. Murray, *Langmuir*, 2009, **25**, 13840.
37 B. J. Plowman, A. P. O'Mullane, P. Selvakannan and S. K. Bhargava, *Chem. Commun.*, 2010, **46**, 9182.
38 J. Zhang, S.-X. Guo, A. M. Bond and F. Marken, *Anal. Chem.*, 2004, **76**, 3619.
39 S. Guo, J. Zhang, D. M. Elton and A. M. Bond, *Anal. Chem.*, 2004, **76**, 166.
40 L. D. Burke, A. P. O'Mullane, V. E. Lodge and M. B. Mooney, *J. Solid State Electrochem.*, 2001, **5**, 319.
41 A. M. Bond, N. W. Duffy, S. X. Guo, J. Zhang and D. Elton, *Anal. Chem.*, 2005, **77**, 186A.
42 P. D. Cobden, B. E. Nieuwenhuys, V. V. Gorodetskii and V. N. Parmon, *Platinum Metals Review*, 1998, **42**, 141.
43 K. Z. Brainina, L. G. Galperin, Y. V. Vikulova, N. Y. Stozhko, A. M. Murzakaev, O. R. Timoshenkova and Y. A. Kotov, *J. Solid State Electrochem.*, 2011, **15**, 1049.
44 O. S. Ivanova and F. P. Zamborini, *J. Am. Chem. Soc.*, 2010, **132**, 70.
45 L. A. Hutton, M. E. Newton, P. R. Unwin and J. V. MacPherson, *Anal. Chem.*, 2011, **83**, 735.
46 D. A. J. Rand and R. Woods, *J. Electroanal. Chem.*, 1971, **31**, 29.
47 J. Zhang, S.-X. Guo and A. M. Bond, *Anal. Chem.*, 2007, **79**, 2276.
48 J. Zhang and A. M. Bond, *J. Electroanal. Chem.*, 2007, **600**, 23.
49 C.-Y. Lee and A. M. Bond, *Langmuir*, 2010, **26**, 16155.
50 A. P. O'Mullane, J. Zhang, A. Brajter-Toth and A. M. Bond, *Anal. Chem.*, 2008, **80**, 4614.
51 B. Lertanantawong, A. P. O'Mullane, W. Surareungchai, M. Somasundrum, L. D. Burke and A. M. Bond, *Langmuir*, 2008, **24**, 2856.
52 J. Rodriguez-Lopez, M. A. Alpuche-Aviles and A. J. Bard, *J. Am. Chem. Soc.*, 2008, **130**, 16985.
53 E. Matveeva, *J. Electrochem. Soc.*, 2005, **152**, H138.
54 L. D. Burke, J. M. Moran and P. F. Nugent, *J. Solid State Electrochem.*, 2003, **7**, 529.
55 L. D. Burke, J. K. Casey, J. A. Morrissey and M. M. Murphy, *Bull. Electrochem.*, 1991, **7**, 506.
56 A. Pearson, A. P. O'Mullane, V. Bansal and S. K. Bhargava, *Chem. Commun.*, 2010, **46**, 731.
57 D. Zhao, Y.-H. Wang, B. Yan and B.-Q. Xu, *J. Phys. Chem. C*, 2009, **113**, 1242.
58 Q.-S. Chen, S.-G. Sun, Z.-Y. Zhou, Y.-X. Chen and S.-B. Deng, *Phys. Chem. Chem. Phys.*, 2008, **10**, 3645.
59 L. Au, X. Lu and Y. Xia, *Adv. Mater.*, 2008, **20**, 2517.
60 J. Chen, B. Wiley, J. McLellan, Y. Xiong, Z. Y. Li and Y. Xia, *Nano Lett.*, 2005, **5**, 2058.
61 I. Najdovski, A. P. O'Mullane and S. K. Bhargava, *Electrochem. Commun.*, 2010, **12**, 1535.
62 R. Woods, in *Electroanalytical Chemistry*, ed. A. J. Bard, Dekker, New York, 1976.
63 V. Bansal, V. Li, A. P. O'Mullane and S. K. Bhargava, *CrystEngComm*, 2010, **12**, 4280.
64 W. Tang, S. Jayaraman, T. F. Jaramillo, G. D. Stucky and E. W. McFarland, *J. Phys. Chem. C*, 2009, **113**, 5014.
65 O. A. Hazzazi, G. A. Attard, P. B. Wells, F. J. Vidal-Iglesias and M. Casadesus, *J. Electroanal. Chem.*, 2009, **625**, 123.
66 J. Zeng, J. Yang, J. Y. Lee and W. Zhou, *J. Phys. Chem. B*, 2006, **110**, 24606.
67 N. Fujiwara, K. A. Friedrich and U. Stimming, *J. Electroanal. Chem.*, 1999, **472**, 120.
68 S. S. Mahapatra, A. Dutta and J. Datta, *Electrochim. Acta*, 2010, **55**, 9097.

 This journal is © The Royal Society of Chemistry 2011